

Macroscopic anisotropy and symmetry breaking in the pyrochlore antiferromagnet $\text{Gd}_2\text{Ti}_2\text{O}_7$ A. K. Hassan,^{1,*} L. P. Lévy,^{1,2} C. Darie,³ and P. Strobel³¹*Grenoble High Magnetic Field Laboratory, MPI-FKF and CNRS, B.P.166, 38042 Grenoble cedex 9, France*²*Institut Universitaire de France and Université J. Fourier, B.P. 41, 38402 St. Martin d'Hères, France*³*Laboratoire de Cristallographie, 25 Ave. des Martyrs, 38042 Grenoble cedex 9, France*

(Received 8 January 2003; published 26 June 2003)

In the Heisenberg antiferromagnet $\text{Gd}_2\text{Ti}_2\text{O}_7$, the exchange interactions are geometrically frustrated by the pyrochlore lattice structure. This ESR study reveals a strong temperature dependent anisotropy with respect to a [111] body diagonal below a temperature $T_A = 80$ K, despite the *spin only* nature of the Gd^{3+} ion. Anisotropy and symmetry breaking can nevertheless appear through the superexchange interaction. In the presence of anisotropic exchanges, short range planar correlations restricted to specific Kagomé planes are sufficient to explain the two ESR modes studied in this work.

DOI: 10.1103/PhysRevB.67.214432

PACS number(s): 75.50.Ee, 75.40.-s, 76.30.Kg

I. INTRODUCTION

In antiferromagnets with competing interactions, no single spin configuration realizes a local energy minimum for all exchange bonds: exchange interactions are “frustrated.” Among all the possible sources of frustration, the most common one has a geometrical origin. On a number of lattices (Kagomé,¹ fcc, pyrochlore²), magnetic ions are located at the vertices of equilateral triangles: the product of exchange interaction on any closed path being negative, these structures are naturally frustrated. In the two-dimensional (2D) Kagomé lattice, equilateral triangles are connected only through their vertices leaving a number of spin degree of freedom unconstrained. Similarly, in the pyrochlore lattice, spins are at the vertices of tetrahedra with equilateral triangular faces. This lattice offers little additional constraints since all the tetrahedra are connected in the 3D structure through their corners. This confers a very high degree of degeneracy to the ground state (GS) manifold: for classical spins, one or more families of continuous rotations leave the energy of any classical ground state unchanged. As a consequence, smaller anisotropic interactions select a particular GS through a mechanism which is specific to the material considered. For example, a variety of ground states have been identified^{2,4} in the pyrochlore family $R_2\text{Ti}_2\text{O}_7$ where the rare earth ions R are antiferromagnetically coupled. The crystal field anisotropy on the rare earth ion R^{3+} plays an important role in the GS selection except for $\text{Gd}_2\text{Ti}_2\text{O}_7$, where the single-ion anisotropy of the *spin-only* $S=7/2$ ion Gd^{3+} ($4f^7$) is weak: $\text{Gd}_2\text{Ti}_2\text{O}_7$ is the only nearly-isotropic Heisenberg pyrochlore antiferromagnet. Frustration depresses its 3D ordering transition which has been observed in specific heat measurements^{3,5} at a temperature $T_c=0.97$ K considerably smaller than the Curie-Weiss (CW) temperature $\theta_{\text{CW}}=-9.9$ K.

The arrangement of the Gd^{3+} magnetic ions in the cubic pyrochlore lattice is shown in Fig. 1. There are two different (111) Gd^{3+} planes perpendicular to a [111] body diagonal. In the “Kagomé” planes, triangular faces of the Gd^{3+} tetrahedra form a two-dimensional Kagomé network of exchange-coupled Gd^{3+} ions (see Fig. 2). These planes are separated by the spins completing the Gd^{3+} tetrahedra: to first order, they are exchange-coupled only to the spins in the Kagomé

planes. According to neutron scattering data,⁴ the Gd^{3+} spins in the Kagomé planes order in a *planar* triangular structure below $T_c=0.97\text{K}$.

In this electron spin resonance (ESR) study, it is shown that the Kagomé planes perpendicular to a *specific* [111] body diagonal are “selected” at temperatures considerably larger than T_c and θ_{CW} . Two strongly temperature dependent resonance lines are observed in the ESR spectrum below a temperature $T_A \approx 80$ K. Their strong angular dependence with respect to a specific $[111] \equiv \hat{n}$ body diagonal identifies a macroscopic anisotropy with respect to this [111] axis. These ESR modes are consistent with noncollinear spin correlations in the Kagomé planes perpendicular to this [111] axis below T_A . This local order is also consistent with the ordered state observed below T_c . The molecular field contributions to the resonant frequencies show that exchange interactions are the source of anisotropy in this material. The observed symmetry breaking below T_A implies that all Gd^{3+} ions no longer interact with the same exchange coupling, and anisotropic forces (dipolar or Dzyaloshinskii-Moriya⁶ exchange or of another origin) are able to select the ground state.

II. EXPERIMENT

The single crystals of $\text{Gd}_2\text{Ti}_2\text{O}_7$ were grown by slow cooling from a molten flux.⁷ Crystals appeared as brown, well shaped octahedra with a $R6=1$ -mm edge. $\text{Gd}_2\text{Ti}_2\text{O}_7$ is an insulator which crystallizes in the cubic, face centered space group $Fd\bar{3}m$ with a lattice constant $a_0=10.184$ Å at room temperature. Only the Gd^{3+} ions possess a magnetic moment $\mu \approx 7.9\mu_B$, close to the free-ion value ($7.94\mu_B$). The measured dc-magnetic susceptibility in a field of $B_{\text{ext}}=0.1$ T has a Curie-Weiss $\chi=C/(T-\theta_{\text{CW}})$ behavior typical of antiferromagnetic interactions with the same $\theta_{\text{CW}}=-9.9$ K previously reported by Raju *et al.*³ The ESR measurements were performed at different frequencies and temperatures using a home built multifrequency high-field ESR spectrometer. Different frequencies were investigated (54 GHz–115 GHz) using back-wave oscillators and Gunn diode sources, guided to the sample with oversized waveguides in a transmission probe. The spectra were recorded as a function of magnetic field at a fixed frequency. In this study, we

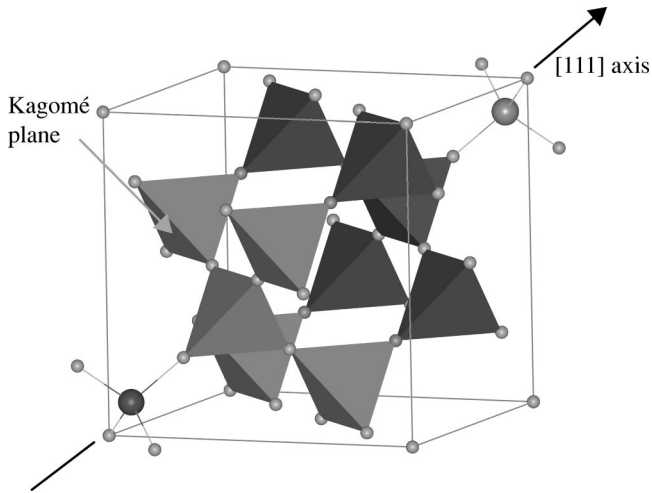


FIG. 1. The Gd^{3+} magnetic ions in the cubic pyrochlore lattice: The ions sit on the vertices of corner sharing tetrahedra. There are two different (111) Gd^{3+} planes perpendicular to a [111] body diagonal. In one of these two planes, the Gd^{3+} ions form a Kagomé network. The pyrochlore lattice can thus be described as a set of 2D Kagomé planes connected by interstitial spins.

have measured (a) the temperature dependence of the ESR spectrum, (b) its orientation dependence with respect to the crystal axes, and (c) its evolution with frequency and magnetic field.

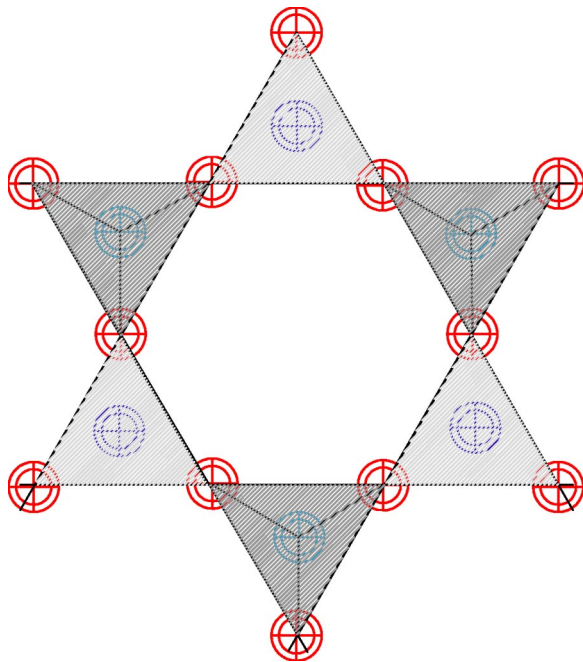


FIG. 2. In the (111) “Kagomé” planes, triangular faces of the Gd^{3+} tetrahedra (the shaded triangles) form a two-dimensional Kagomé network of exchange-coupled Gd^{3+} ions (represented by circles placed on the corners of the shaded triangles). These planes are separated by the “interstitial” spins completing the Gd^{3+} tetrahedra (represented by circles above and below the centers of the shaded triangles).

III. RESULTS AND DISCUSSION

Above 80 K, the ESR spectrum of $\text{Gd}_2\text{Ti}_2\text{O}_7$ at the frequency of 54 GHz consists of a single line centered at $B_r \approx 2$ T, close to the expected resonance field (1.93 T) for a g factor of 2 (as expected for the *spin-only* Gd^{3+}). As the temperature is lowered, two resonance lines appear below $T_A \approx 80$ K. Their splitting is strongly anisotropic and temperature dependent, and becomes comparable to the spin-exchange frequencies ($4 \text{ T} \equiv 5.4 \text{ K}$) at low temperature. This is represented in Fig. 3, which shows the ESR spectra at 54 GHz for different temperatures, with the magnetic field applied parallel to a specific body diagonal of the crystal ($[111] \equiv \hat{n}$ axis, perpendicular to Kagomé planes), such that the angle $\theta = \angle(\vec{B}, \hat{n}) = 0$. Fitting the spectra below 80 K with two Lorentzian lines (1) and (2), the position of the resonance fields can be plotted as a function of temperature. Line (2) is strongly temperature dependent as clearly seen in Fig. 3(b). Its resonance field shifts towards higher values as the temperature is decreased, the shift being very large (~ 4 T) at low temperature (4.2 K). As the line shifts, a broadening is also observed. While the width of line (1) also increases when lowering the temperature, the line shift is much weaker: its resonance field moves towards lower values, the change being of the order of 0.3 T at 4.2 K. On the other hand, when the magnetic field is applied perpendicular to the

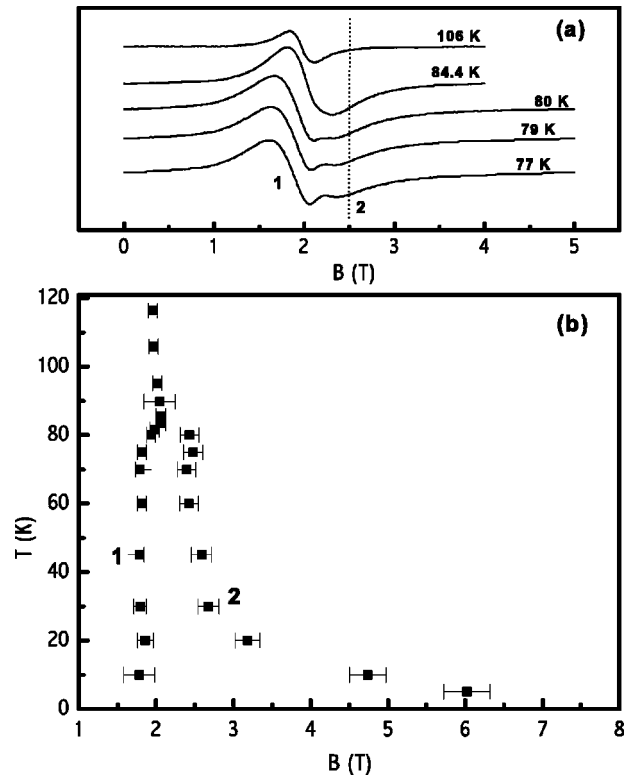


FIG. 3. (a) ESR spectra in the vicinity of the temperature T_A taken at 54 GHz with the magnetic field applied parallel to the [111] axis. The dotted line specifies the position of line 2 at 77 K after deconvolution of the line shape into two Lorentzians. (b) Temperature dependence of the positions of lines 1 and 2 in the same experimental conditions. At 4 K, the splitting between the two lines ($4 \text{ T} \equiv 5.4 \text{ K}$) becomes comparable to θ_{CW} .

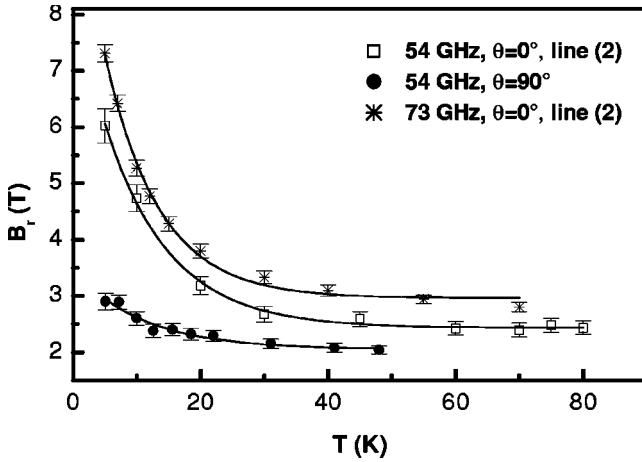


FIG. 4. Temperature dependence of the resonance fields. The solid lines are fits according to the expression $B_r(T) = B_0 + D \exp(-T/T_0)$. The obtained values of T_0 are 10.1 ± 0.5 K (10.8 ± 2.1 K) at 54 GHz for $\theta=0$ ($\theta=90^\circ$), and 8.5 ± 0.5 K at 73 GHz for $\theta=0$. At 54 GHz and $\theta=90^\circ$ only one line is observed.

body diagonal \hat{n} (i.e., $\theta=90^\circ$), at the same frequency 54 GHz, the position of the observed signal also shifts to higher fields with decreasing temperature, but the shift is smaller, ~ 1 T at 4.2 K.

Although there is no long range order at the temperatures studied in this work, the large temperature dependence of the position of line (2) reveals the presence of an internal field at the frequencies probed in the experiment. The presence of local fields signals the growth of short range spin correlations as the temperature is lowered. Roughly speaking, when the local field \vec{h}_i is not collinear with the local magnetization $\langle \vec{S}_i \rangle$, the resultant torque adds to or subtracts from the Larmor term and produces a shift of the resonant field (or frequency). In the presence of short range spin correlations, \vec{h}_i and $\langle \vec{S}_i \rangle$ are not parallel if one or both of the following situations is encountered: (i) spin correlations are noncollinear, and (ii) the exchange interactions are anisotropic.

Since local fields fluctuations on time scales faster than the precession period average to zero, then the observed frequency shifts decrease with increasing temperature on a scale characteristic of the short range spin dynamics. Considering that spin correlations $\langle S_i S_j \rangle \propto \exp(-|r_i - r_j|/\xi)$ have an exponential dependence with the correlation length ξ , it is instructive to compare the temperature dependence of the observed shifts to exponential functions of temperature. The temperature dependence of the resonance fields below 80 K is shown in Fig. 4 for (i) both orientations $\theta=0$ and $\theta=90^\circ$ at 54 GHz, and (ii) for $\theta=0$ at 73 GHz. The solid lines are fits to the phenomenological expression $B_r(T) = B_0 + D \exp(-T/T_0)$, (where B_0 is the resonance field at high temperature and D a parameter), consistent with an activated behavior with an activation energy $k_B T_0$. From the fits, the obtained values of T_0 are 10.1 ± 0.5 K (10.8 ± 2.1 K at 54 GHz for $\theta=0$ ($\theta=90^\circ$), and 8.5 ± 0.5 K at 73 GHz for $\theta=0$). These values are comparable to the Curie-Weiss temperature, $\theta_{CW} \approx -10$ K. This shows that the origin of the observed shift is related to an exchange mechanism and is thus magnetic.

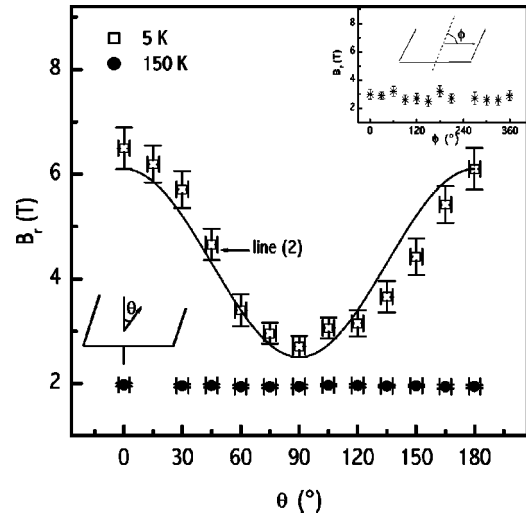


FIG. 5. Orientation dependence of line (2), studied at the frequency 54 GHz, as the magnetic field is rotated away from the [111] axis into the (111) plane. The strong dependence observed at 4.5 K can be fitted to $B_r^0 + D \cos^2 \theta$ with $B_r^0 = 2.5$ T and $D = 3.6$ T. When $\theta=90^\circ$, lines (1) and (2) merge together at 54 GHz. The inset shows a complete rotation in the plane. At 150 K, the single resonance observed is independent of the orientation of the magnetic field.

In order to investigate further the nature of this local order, we studied the orientation dependence of the ESR modes of our single crystal. A plot of the resonant fields versus the angle θ between the applied magnetic field and the body diagonal \hat{n} is shown in Fig. 5, at a fixed frequency (54 GHz) and for two different temperatures, 150 and 4.5 K. The single resonance observed at 150 K is independent of the magnetic field orientation and therefore isotropic. However at 4.5 K, the position of resonance (2) has a strong dependence on the field direction. As the magnetic field is rotated away from the [111] direction of the crystal, the resonance position decreases until it reaches a minimum at $\theta=90^\circ$ and recovers its $\theta=0$ value as the field is rotated towards 180° with respect to the [111] direction. Hence, the anisotropy has a uniaxial character, with an angular dependence for the resonance field $B_r^{(2)}(\theta) = B_r^0 + D \cos^2 \theta$ (with $B_r^0 = 2.5$ T and $D = 3.6$ T). This minimum in the resonance field B_r^0 occurs when the magnetic field is in the (111) Kagomé plane $\perp \hat{n}$. This singles out a unique anisotropy axis and establishes the macroscopic nature of the anisotropy. This is further evidenced by the inset of Fig. 5, where a complete rotation ϕ in that plane is presented. The dependence of the resonance fields on the orientation of the magnetic field is weaker, $\Delta B_{r,\max} \sim 0.7$ T, and may be attributed to dipolar and/or demagnetization effects.

The frequency dependence of resonances (1) and (2) has been studied at $T=4.5$ K for two different orientations of the magnetic field, parallel ($\theta=0^\circ$, perpendicular to the Kagomé-plane) and perpendicular ($\theta=90^\circ$, in the Kagomé plane) to the body diagonal (\hat{n}). This frequency dependence is shown as a function of magnetic field in Fig. 6. The frequency dependence of line (1) goes through the origin and is linear with magnetic field ($\omega_1 = \gamma H$) with a gyromagnetic ratio close to $\gamma \approx \mu/\hbar$: this is the uniform precession mode. On the other hand, line (2) has a different field dependence.⁸ Con-

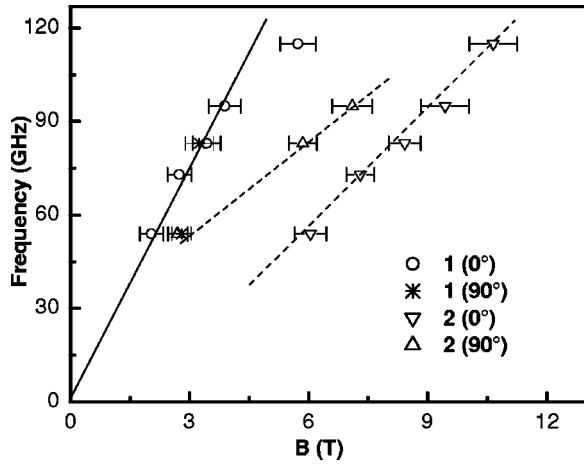


FIG. 6. The frequency vs field diagram for resonances (1) and (2) at 4.5 K, parallel ($\theta=0^\circ$) and perpendicular ($\theta=90^\circ$) to the body diagonal \hat{n} ([111]). The lines are guides to the eye.

sidering the nature of the observed anisotropy, the spins in the (111) Kagomé planes are not magnetically equivalent to the spins in between them. In these circumstances, the presence of two lines in the ESR spectrum is not really surprising,⁹ especially if we consider the short range order present at the temperature of the measurement ($T=4.5$ K). At 4.5 K the exchange fields h_i and h_b for spins in (i) and in between (b) the Kagomé planes are comparable to the applied magnetic fields H and $k_B T$. The collective modes observed in ESR are always the linearized modes for the deviations δm_i (respectively, δm_b) of the local magnetization in (respectively, in between) the Kagomé planes from their equilibrium. In the presence of any exchange anisotropies, the local fields $h_{i,b} \neq m_{i,b}/\chi - H$ contribute to the ESR frequency shifts from the Larmor precession mode. The shifts are further enhanced by the noncollinear spin correlations which develop at low temperature.

The main experimental findings may be summarized as follows: below T_A , a macroscopic anisotropy appears with respect to a broken symmetry axis \hat{n} lying along a *specific* body diagonal of the crystal. This macroscopic character has been checked through dc-torque measurements.¹⁰ This anisotropy develops gradually as the local order (due to short range correlations) sets in when the temperature is lowered. This is illustrated in Fig. 7, where the difference between the resonance fields of line (2) for $\theta=0^\circ$ and $\theta=90^\circ$ is plotted versus the temperature. Anisotropies of local origin, such as the g factor and single ion, are usually unaffected by spin correlations and thus temperature independent. Below the ordering temperature at $T_c=0.97$ K, the structure of the ordered state has been identified in a neutron scattering experiment⁴ with an isotope enriched $^{160}\text{Gd}_2\text{Ti}_2\text{O}_7$ sample: within the Kagomé plane, spins are ordered in a chiral 120° structure (identical to the “ $q=0$ ” spin structure observed in ordered Kagomé antiferromagnets¹¹), while the structure for the spins in between the planes has not been definitively established. This structure is fully consistent with the anisotropic local order observed here at higher temperatures. Mössbauer experiments also show that, below T_c , the or-

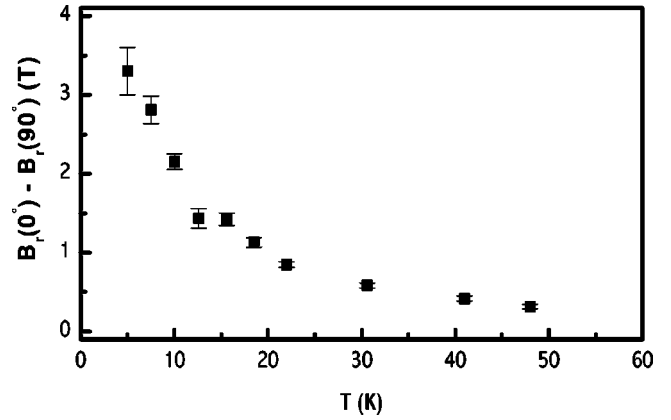


FIG. 7. Difference in resonance field for line (2) for a field along and perpendicular to the anisotropy axis \hat{n} .

dered magnetic moment at each Gd site is perpendicular to the local (111) axis.¹²

We first consider the microscopic forces which could give rise to this macroscopic anisotropy with respect to a specific body diagonal. Let us first consider the main superexchange interaction between neighboring Gd^{3+} ions. Two oxygen ions bridge the vertices of the tetrahedral Gd^{3+} pyramid. The shortest bridge goes through the oxygen located in the center of the tetrahedron, which bridges *all* four Gd^{3+} ions at the tetrahedron vertices. We focus on this shortest bridge. If only the strong ligand electric fields are considered, the four oxygen orbitals are identical sp^3 mixtures pointing toward the tetrahedron vertices. In a T_d symmetry, the Hund term on the oxygen splits the four sp^3 orbitals into a singlet and a triplet. This energy splitting will reduce the superexchange coupling between the Gd^{3+} ion coupled to this singlet sp^3 oxygen orbital with respect to all other three Gd^{3+} ions. An alternative scenario would involve a motion of the oxygen in the center of each tetrahedron. On the other hand, there are no experimental evidence so far of a structural transition around 80 K or higher. The mechanisms just described do not produce, by themselves, a spin anisotropy. However, the Dzyaloshinskii-Moryia exchange interactions⁶ will provide in this circumstance a macroscopic coupling $D_{DM}^i \hat{n} \cdot \vec{S}_i \times \vec{S}_j$ for the spins \vec{S}_i and \vec{S}_j in the Kagomé plane and an anisotropy in the exchange constants. For a pure Kagomé lattice, these terms are known¹³ to give rise to the same chiral order as observed by neutron scattering.⁴ Dipolar interactions¹⁴ could also favor such a state, once the spins are restricted to the Kagomé planes. In order to experimentally validate this scenario, the knowledge of the magnetic structure for the different magnetic phases in a magnetic field⁵ would be decisive.

Whether this exchange mechanism plays a significant role in other pyrochlore magnets with large single-ion anisotropies is also open. For example, in the $\text{Tb}_2\text{Ti}_2\text{O}_7$ pyrochlore, the crystal field splitting of the Tb^{3+} ion is estimated to be in the 15–20 K range,¹⁵ which is far less than the temperature (50 K) where short range order sets in Ref 16. In such circumstances, an exchange-driven anisotropy could be important.

The results of our experiment also specify the minimal ingredients which need to be included in a phenomenological model describing $\text{Gd}_2\text{Ti}_2\text{O}_7$. Spins in (i) and in between (b) Kagomé planes are considered as inequivalent below T_A : their local magnetizations m_i and m_b need to be treated separately. Furthermore, a source of anisotropic exchange has to be introduced in the model. Combining these two assumptions, the data presented in this work can be very nicely described.¹⁷

IV. CONCLUSION

This ESR study has revealed an unexpectedly large magnetic anisotropy for a pyrochlore magnet with spin-only

Gd^{3+} ions. The observed ESR modes, in particular their evolution with temperature, frequency, and magnetic field orientation, are also consistent with non-collinear spin correlations in the Kagomé planes perpendicular to a specific [111] body diagonal. The possible exchange driven nature of the found anisotropy stresses the importance of the subtleties of the microscopic coupling between the rare earth ions in these frustrated magnets where a large degree of degeneracy is present.

ACKNOWLEDGMENTS

We gratefully acknowledge very helpful discussions with B. Canals, M. Elhajal, C. Lacroix, and A. Wills.

*Corresponding author: Email address: hassan@polycnrs-gre.fr

¹K. Kano and S. Naya, *Prog. Theor. Phys.* **10**, 158 (1953).

²A.P. Ramirez, *Annu. Rev. Nucl. Sci.* **24**, 452 (1993).

³N.P. Raju, M. Dion, M.J.P. Gingras, T.E. Mason, and J.E. Greedan, *Phys. Rev. B* **59**, 14 489 (1999).

⁴J.D.M. Champion, A.S. Wills, T. Fennell, S.T. Bramwell, J.S. Gardner, and M.A. Green, *Phys. Rev. B* **64**, 140407 (2001).

⁵A.P. Ramirez, B.S. Shastry, A. Hayashi, J.J. Krajewski, D.A. Huse, and R.J. Cava, *Phys. Rev. Lett.* **89**, 067202 (2002).

⁶I.E. Dzyaloshinskii, *Zh. Éksp. Teor. Fiz.* **32**, 1547 (1957) [*Sov. Phys. JETP* **5**, 1259 (1957)]; T. Moriya, *Phys. Rev.* **120**, 91 (1960).

⁷B.M. Wanklyn and A. Maqsood, *J. Mater. Sci.* **14**, 1975 (1979).

⁸We have tried to follow the dependence of line 1 and 2 to lower frequencies (X band), but their broadening becomes so large that it is extremely difficult to determine their position with sufficient precision.

⁹The presence of two lines in the ESR spectrum, in the absence of long range order has been observed in other systems, such as

spin glasses: S. Schultz, E.M. Gullikson, D.R. Fredkin, and M. Tovar, *Phys. Rev. Lett.* **45**, 1508 (1980).

¹⁰The results of the dc torque measurements will be published elsewhere.

¹¹J.N. Reimers and A.J. Berlinsky, *Phys. Rev. B* **48**, 9539 (1993).

¹²E. Bertin, P. Bonville, J.P. Bouchaud, J.A. Hodges, J.P. Sanchez, and P. Vulliet, *Eur. Phys. J. B* **27**, 347 (2002).

¹³M. Elhajal, B. Canals, and C. Lacroix, *Phys. Rev. B* **66**, 014422 (2002).

¹⁴S.E. Palmer and J.T. Chalker, *Phys. Rev. B* **62**, 488 (2000).

¹⁵M.J.P. Gingras, B.C. den Hertog, M. Faucher, J.S. Gardner, S.R. Dunsiger, L.J. Chang, B.D. Gaulin, N.P. Raju, and J.E. Greedan, *Phys. Rev. B* **62**, 6496 (2000).

¹⁶J.S. Gardner, S.R. Dunsiger, B.D. Gaulin, M.J.P. Gingras, J.E. Greedan, R.F. Kiefl, M.D. Lumsden, W.A. MacFarlane, N.P. Raju, J.E. Sonier, I. Swainson, and Z. Tun, *Phys. Rev. Lett.* **82**, 1012 (1999).

¹⁷A. Hassan and L.P. Lévy (unpublished).